Analytica Chimica Acta 1082 (2019) 116–125

Contents lists available at ScienceDirect

Analytica Chimica Acta

journal homepage: www.elsevier.com/locate/aca

A twist six-membered rhodamine-based fluorescent probe for hypochlorite detection in water and lysosomes of living cells

Zechen Wang [a, 1], Qinghao Zhang [a, 1], Junwen Liu [a, 1], Ran Sui [a], Yahui Li [a], Yue Li [a], Xinfu Zhang [b], Haibo Yu [a, *], Kui Jing [a, **], Mingyan Zhang [c], Yi Xiao [b, ***]

[a] College of Environmental Sciences, Liaoning University, Shenyang, 110036, PR China
[b] State Key Laboratory of Fine Chemicals, Dalian University of Technology, Dalian, 116024, PR China
[c] Liaoning Center of Disease Prevention and Control, Shenyang, 110001, PR China

HIGHLIGHTS

- A twist six-membered rhodamine fluorescent probe 6G-ClO has been developed with the precursor 2-formyl-rhodamine 6G.
- 6G-ClO bearing unique six-membered spirocycle is characterized by NMR and HRMS spectra.
- 6G-ClO exhibits high sensitivity and fast response to ClO^- in real water samples.
- The detection limit of 6G-ClO was as low as 12 nM for ClO^-.
- 6G-ClO localizes specifically in lysosomes and monitors exogenous and endogenous ClO^- in live HUVEC cells.

GRAPHICAL ABSTRACT

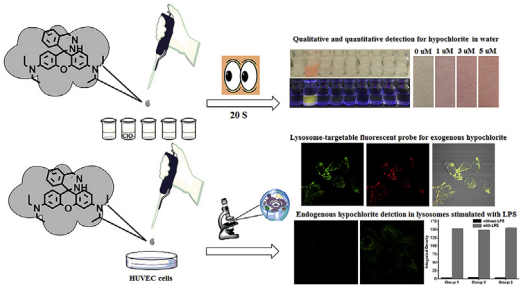

ARTICLE INFO

Article history:
Received 16 April 2019
Received in revised form
24 June 2019
Accepted 23 July 2019
Available online 26 July 2019

Keywords:
Fluorescent probe
Six-membered rhodamine
Hypochlorite detection
Lysosome-targetable
Living cells

ABSTRACT

A novel six-membered rhodamine-based fluorescent probe (6G-ClO) was developed from 2-formyl rhodamine (6G-CHO) and used for hypochlorite detection in water and HUVEC cells. Different from planar penta cycle of rhodamine spirolactam, there was a twist six-membered spirocyclic hydrazone in 6G-ClO optimized by Gaussian software at DFT/B3LYP/6-31G(d) level. The high selectivity, high sensitivity and fast response of 6G-ClO towards ClO^- would be attributed to the twist six-membered spirocycle. Test-strip prepared with 6G-ClO was successfully used to semi-quantitatively indicate the concentration of ClO^- in water. 6G-ClO can also quantitatively detect the concentration of ClO^- in tap water and swimming pool water. The detection limit of 6G-ClO was as low as 12 nM. The co-localization staining of HUVEC cells further verified that 6G-ClO could specifically accumulate in lysosomes and capture exogenous/endogenous ClO^- in living lysosomes. 6G-ClO would be a practical probe for real-time monitoring of ClO^- in the biological and real water samples.

1. Introduction

Hypochlorite salts, known as the germicidal ability and oxidation, are widely utilized in various occasions including drinking water treatment [1,2], pollutant elimination [3–5], wound

* Corresponding author.
** Corresponding author.
*** Corresponding author.
E-mail address: yuhaibo@lnu.edu.cn (H. Yu).
[1] These authors contributed equally to this work.

https://doi.org/10.1016/j.aca.2019.07.046
0003-2670/

disinfection [6,7] and endodontic irrigation [8,9]. Over one hundred years later, hypochlorite has been still in use, attributing to its residual protection, low cost and ease of use [10,11]. Considering the risk of chlorine gas, sodium hypochlorite has been an optimal alternative as disinfectants for many water treatment facilities in recent years [12,13]. However, improper storage and usage of sodium hypochlorite will result in toxic disinfection by-products (DBPs) such as chlorate, perchlorate and trihalomethanes, to be generated in drinking water disinfection [14,15]. Ultimately, those DBPs entering human body through water and food intake may cause fetal malformation [16], hormonal disorders [17] and the breakdown of red blood cells [12]. Therefore, a reasonable usage of hypochlorite will be of great significance for risk management in water disinfection. Hypochlorite is not solely an oxidant consumed in industry and medicine surgery, but exists as endogenous reactive oxygen species (ROS) and plays a critical role in inflammatory stress of human body. Endogenous hypochlorous acid and hypochlorite ($HClO/ClO^-$) are now known to be generated from H_2O_2 and chloride ions Cl^- in the presence of myeloperoxidase (MPO) [18,19]. The disorder of MPO would endogenously produce superfluous hypochlorite, which further leads to oxidation damage of protein, amino acids, peptide and lipid [20,21]. Hypochlorite is believed to involve in many diseases, e. g. arthritis [22], kidney disease [23], lung injury [24], atherosclerosis [25], and cancer [26]. Considering the health risk of hypochlorite, it is necessary to quantitatively and qualitatively monitor hypochlorite both in real water samples and in biological specimens.

To determine hypochlorite in different situation, up to now a lot of fluorescent probes have been reported and applied for hypochlorite in solution and living cells [27–38]. Rhodamine-based probe, as the most typical one of them, is developing most rapidly in the recent years, owing to its excellent switching properties of five-membered spirolactam [39–48]. The colorless and non-fluorescent five-membered spirolactam with low signal background can be transformed into a ring-opening zwitterion with intensive absorptions and emissions by analytes. The switching nature makes rhodamine spirolactam popular in the fields of colorimetric chemosensors [49,50], thermochromatic materials [51], super-resolution bioimaging [52–54], and so on. Of late six-membered rhodamine spirocycles used as fluorescent probe for metal ions arrests our attention [55–59]. Compared with five-membered spirolactam, the expandation of spirocycle might be helpful to improve the selectivity and sensitivity of fluorescent probe for analytes [59]. Yet until now, only five six-membered rhodamine spirocycles have been reported as chemosensors for Hg^{2+} or Cu^{2+} monitoring (Scheme 1a). To deeply understand the switching properties of six-membered spirocycle, developing new six-membered spirocyclic rhodamine for hypochlorite detection is still highly demanded yet challenging.

The success of rhodamine spirolactams as chemosensors is due to its platform status possessing the unique reaction of 2-carboxyl rhodamine with amines, which will be of inspired meaning to develop six-membered rhodamine spirocycles for hypochlorite detection. To enrich six-membered rhodamine spirocycle, herein, 2-aldehyde rhodamine (6G-CHO) was firstly developed and used as a scaffold to design six-membered rhodamine spirocyclic hydrazone (6G-ClO) for hypochlorite detection (Scheme 1b). To the best of our knowledge, 6G-ClO was the first colorimetric and fluorometric probe for hypochlorite based on six-membered rhodamine spirocycle. Rhodamine 6G spiroaminoethanol (6G-SAE) was obtained from rhodamine 6G and aminoethanol in DMF. Via a reduction reaction of 6G-SAE with $LiAlH_4$, 2-aldehyl-rhodamine 6G (6G-CHO) was prepared in 20% yield. Finally, probe 6G-ClO was easily generated from the reaction between 6G-CHO and hydrazine hydrate in 58% yield. The six-membered spirocycle in 6G-ClO was further verified by the chemical shift of spiro-carbon (δ_C 94.9 ppm) and −CH=N−NH (δ_{CH} 8.03 ppm; δ_{NH} 6.51 ppm) in NMR spectra, respectively.

2. Experimental section

2.1. Materials and methods

Rhodamine 6G, ethanolamine and $LiAlH_4$ were purchased from Aladdin (Shanghai, China). 80% Hydrazine hydrate and triethylamine was supplied by Sinopharm Chemical Reagent Co. Ltd (China). 2-[4-(2-Hydroxyethyl)-1-piperazinyl]ethanesulfonicacid (HEPES) was purchased from Huaxia Reagent Co. Ltd (Chengdu, China). The solvents including THF, C_2H_5OH, DMF and CH_2Cl_2 were obtained from commercial supplier. Column chromatography was performed with silica gel (300–400 mesh). HUVEC (Human umbilical vein endothelial cells) were obtained from Institute of Basic Medical Sciences (IBMS) of Chinese Academy of Medical Sciences (CAMS). RPMI (Roswell Park Memorial Institute) 1640, Mito-tracker Deep Red and Lyso-tracker DND-26 were purchased from ThermoFisher (Invitrogen).

2.2. Synthesis of 6G-CHO

Ethanolamine (500 μL, 8.35 mmol) was added into a solution of rhodamine 6G (1 g, 2.09 mmol) in 30 mL DMF, and then triethylamine (1.16 mL, 8.35 mmol) was added dropwise. The mixture was stirred and heated at 100 °C for 10 h. After the DMF was removed under vacuum, the residue was poured into ice water. Crude product (6G-SAE) was filtered and used without further purification. 6G-SAE (100 mg, 0.219 mmol) in anhydrous THF was stirred at room temperature in the presence of $LiAlH_4$ (25 mg, 0.659 mmol). After 30 min, 5 mL THF without dehydration was supplemented and stirred for half an hour. Then 17 mg (0.448 mmol) of $LiAlH_4$ was added and stirred overnight. The reaction solution was quenched carefully with 1 mL of deionized water. The product (17 mg) was purified by column chromatography (DCM: MeOH, 10: 1, v:v) to give 6G-CHO in 20% yield. HRMS called 399.2067, found 399.2066, ^{1}H NMR (300 MHz, DMSO) δ 9.83 (s, 1 H), 8.26 (d, J = 9.0 Hz, 1 H), 8.07–7.88 (m, 2 H), 7.79 (s, 2 H), 7.51 (d, J = 6.0 Hz, 1 H), 6.94 (s, 2 H), 6.79 (s, 2 H), 3.51 (s, 4 H), 2.09 (s, 6 H), 1.26 (t, J = 6.0 Hz, 6 H). ^{13}C NMR (75 MHz, DMSO) δ 192.1, 156.8, 155.9, 154.8, 134.5, 133.3, 132.2, 130.7, 130.5, 128.5, 125.6, 113.4, 93.7, 38.0, 17.5, 13.7.

2.3. Synthesis of 6G-ClO

6G-CHO (50 mg, 0.125 mmol) was dissolved in absolute ethanol (30 mL) in a round bottom flask, and then 1 mL of hydrazine hydrate was added dropwise into the solution. The reaction was refluxed for 2 h. During this process, the solution color changed colorless from pink. After the solvent was removed under vacuum, 6G-ClO (30 mg) was obtained by column chromatography (DCM: MeOH, 100: 1, v:v), yield 58%. HRMS $[M+H]^+$ called 413.2341, found 413.2326, ^{1}H NMR (500 MHz, DMSO) δ 8.03 (s, 1 H), 7.18–7.10 (m, 4 H), 6.94 (s, 2 H), 6.51 (d, J = 5.0 Hz, 1 H), 6.16 (s, 2 H), 4.92 (t, J = 5.0 Hz, 2 H), 3.10 (q, J = 5.0 Hz, 4 H), 1.94 (s, 6 H), 1.20 (t, J = 5.0 Hz, 6 H). ^{13}C NMR (125 MHz, DMSO) δ 147.9, 146.9, 137.5, 130.1, 129.7, 129.5, 127.4, 126.9, 124.3, 123.1, 117.3, 115.2, 94.9, 53.7, 37.5, 17.2, 14.2.

2.4. Preparation of the test solutions and spectral measurements

4.13 mg 6G-ClO was dissolved in 10 mL dichloromethane in volumetric flask. The concentration of stock solution of 6G-ClO was 1×10^{-3} mol/L. During spectral detection, 2 mL stock solution

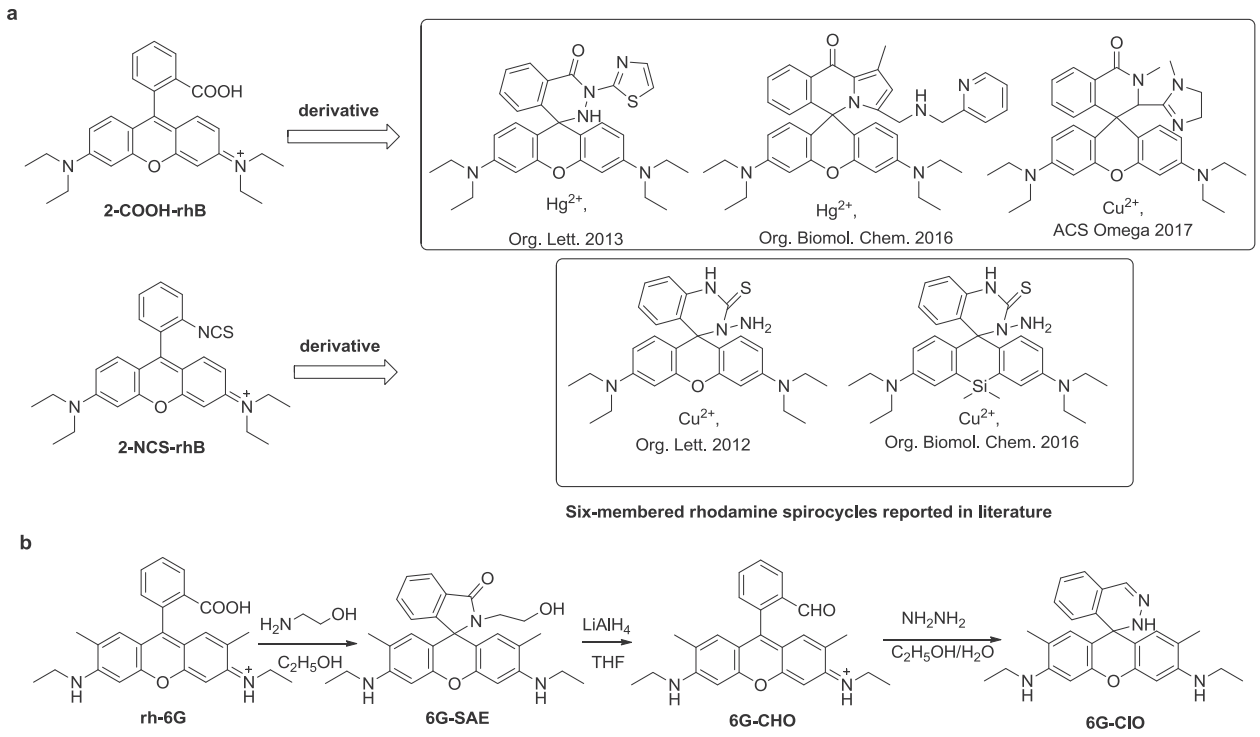

Scheme 1. (a) Six-membered rhodamine spirocycles and its precursors reported in literature. (b) Synthetic route of new six-membered rhodamine spirocycle 6G-ClO in this work.

(1×10^{-3} mol/L) was added into a 100 mL volumetric flask, and the solvent (CH_2Cl_2) was removed. Then a mixture of ethanol and 20 mM HEPES (v:v, 1:1, pH 7.4) was poured into the flask to obtain test solution (2×10^{-5} mol/L). After a certain amount of analytes was added into the test solution, the absorption and emission spectra of 6G-ClO were recorded in UV–vis spectrophotometer and fluorescence spectrophotometer, respectively.

2.5. The calibration of ClO^- solution

The calibration of NaClO solution was referred the methods reported in literature [60,61]. In these methods, 10 mL tested hypochlorite sodium was firstly injected into a volumetric flask (100 mL), then deionized water was added. Shake well and place it in the dark. Next, 10 mL above hypochlorite sodium solution was further diluted with 100 mL deionized water in 250 mL iodine flask. Then 10 mL KI (100 g/L) solution and 10 mL dilute H_2SO_4 (0.552 mol/L) was added into the above flask. Shake well and seal with water in the dark for 5 min. Finally, $Na_2S_2O_3$ was used to calibrate the concentration of hypochlorite sodium in the presence of starch as an indicator.

2.6. Qualitatively and quantitatively detection of ClO^- solution

6G-ClO was added into different vials with a kind of anion water solution. If the color of solution changed pink from colorless and its fluorescence turned on, it can be confirmed qualitatively that the solution in this vial contained a certain amount of hypochlorite anion. The quantity of hypochlorite can be assessed, according to the standard curve.

2.7. Exogenous and endogenous hypochlorite detection

HUVEC cells were incubated with 6G-ClO (5 μM, containing 0.1% DMSO in PBS) at 37 °C for 10 min. After washed with PBS twice, cells were treated with 100 μM NaClO for 10 min. Then the images for exogenous hypochlorite were obtained from the microscope. In order to detect endogenous hypochlorite, LPS was used as a stimulant in the cells incubation. In control groups, cells were incubated with 6G-ClO at 37 °C for 10 min and washed with PBS three times. 3 mL 1640 without FBS was added and incubated at 37 °C for 24 h. In experimental groups, after cells were incubated with 6G-ClO and washed with PBS three times, LPS (2 μg/mL in 3 mL RPMI 1640 without FBS) was added and further incubated at 37 °C for 24 h.

3. Results and discussion

3.1. The design and synthesis of 6G-ClO

Comparison of the existing six-membered rhodamine spirocycles, it was not difficult to find that there was a reactive group in 2-position of rhodamine dyes. Up to now, only two rhodamine precursors, 2-carboxyl rhodamine B (2-COOH-rhB) and 2-isothiocynate or 2-amino-rhodamine B (2-NCS-rhB or 2-NH_2-rhB), have been successfully used to synthesize six-membered rhodamine spirocycles, as shown in Scheme 1a. To construct new six-membered rhodamine spirocycles, novel rhodamine intermediate bearing active group in 2-position was in a great demand. Aldehyde group is well known for its reactivity in many kinds of reactions, including Schiff base reaction, Knoevenagel condensation, Wittig reaction, and so on. It has be verified that 2-formyl rhodamine would be a critical candidate for fluorescent probes based on rhodamine dyes [62–64]. Then, 2-formyl rhodamine 6G was chosen as an intermediate to synthesize six-membered rhodamine spirocyclic hydrazone (Scheme 1b). The structure of 6G-CHO was characterized by HRMS m/z 399.2066 and NMR in which the chemical shifts of aldehyde group were 9.83 (δ_H) ppm and 192.1 (δ_C) ppm, respectively. Probe 6G-ClO was easily produced from the reaction between 6G-CHO and hydrazine hydrate in ethanol.

3.2. Geometry optimization

In order to test this hypothesis, the geometry of 6G-ClO with six-membered spirocycle was optimized by Gaussian software at DFT/B3LYP/6-31G(d) level (Fig. 1). In contrast, rhodamine 6G acylhydrazine (6G-AH) was also optimized in the same basic set (Fig. S1). Different from planar penta cycle of 6G-AH, there was a non-planar six-membered rhodamine spirocyclic hydrazone in 6G-ClO. The dihedral angles C1–N2–N3–C4 (−15.6°) and C5–C6–C1–N2 (−16.5°) indicated that there was a twist six-membered ring, due to tetrahedral geometry resulting from sp^3 hybridized NH in hydrazone moiety. The dihedral angles C5–C6–C1–C7 (103.5°) and C5–C6–C1–C8 (−133.6°) suggested that the benzene ring in dihydrophthalazine moiety was not perpendicular to the xanthene ring in 6G-ClO. The bond angles C6–C1–N2 and N3–N2–C1 were 107.3° and 127.6°, which were higher than that of 6G-AH. These results suggested that there was a stronger ring strain for six-membered spirocyclic hydrazone in 6G-ClO, compared with 6G-AH. Additionally, the electron distributions in HOMO and LUMO of 6G-ClO were illuminated in Fig. 1. In HOMO orbital of 6G-ClO the electron was delocalized on xanthene ring and dihydrophthalazine moiety, whereas the electron of 6G-AH in HOMO was distributed primarily on xanthene ring moiety (Fig. S1). Compared with 6G-AH, the higher electron density of hydrazone moiety in 6G-ClO would be more vulnerable to hypochlorite, which would serve the high sensitivity and fast response towards ClO^-.

3.3. Spectral selectivity of 6G-ClO toward analytes

The optical properties of 6G-ClO toward various analytes were studied in aqueous solution (C_2H_5OH/HEPES, pH 7.4). As shown in Fig. 2, the absorption and emission intensities of 6G-ClO were faint in the absence of ClO^-. Upon addition of 5 equiv. ClO^-, a new absorption peak arose at 533 nm and a visible pink color of 6G-ClO solution appeared immediately (Fig. 2a). Meanwhile, an enhancing fluorescence of 6G-ClO observed at the maximum of emission (556 nm, Fig. 2b) indicated that a ring-opening reaction of six-membered spirocyclic hydrazone could be induced by hypochlorite anion. However, the absorption and emission spectra of 6G-ClO did not changed upon addition of 5 equiv. anions and other analytes including $ONOO^-$, Cl^-, HPO_4^{2-}, $H_2PO_4^-$, SO_4^{2-}, NO_3^-, CO_3^{2-}, $S_2O_3^{2-}$, H_2O_2, NO_2^-, ·OH, F^-, Br^-, I^-, CN^-, SO_3^{2-}, NO and H_2S. Moreover, the enhancement of absorption and emission intensity resulting from the addition of ClO^- was fulfilled, even if the other anions were added firstly (Fig. 2c and d). In addition, the interferences of metal ions towards 6G-ClO were also investigated in C_2H_5OH/HEPES (pH 7.4). There were no observable spectral changes upon addition of 5 equiv. various metal ions, e. g. K^+, Ca^{2+}, Na^+, Mg^{2+}, Fe^{2+}, Zn^{2+}, Al^{3+}, Cd^{2+}, Cr^{3+}, Hg^{2+}, Mn^{2+}, Fe^{3+}, Cu^{2+} (Fig. S2). In order to demonstrate the high selectivity of 6G-ClO for hypochlorite, rhodamine 6G acylhydrazine (6G-AH) was synthesized as a control compound and its spectral selectivity for various analytes was studied (Fig. S2). Both ClO^- and NO could induce a ring-opening reaction of five-membered spirolactam in 6G-AH. Upon addition of above metal ions into 6G-AH solution, Hg^{2+} can cause a significant color change of the solution. Compared with 6G-AH, probe 6G-ClO exhibited a higher selectivity towards hypochlorite than other anions and metal ions.

3.4. Spectral response of 6G-ClO to ClO^-

The spectral responses of 6G-ClO towards ClO^- in C_2H_5OH/HEPES (pH 7.4) were carried out and recorded in UV–Vis spectrophotometer and fluorophotometer. As shown in Fig. 3, with increasing of ClO^-, the absorption intensity increased gradually, while the pink color of solution became dark accordingly (Fig. 3a). Corresponding with the concentration of ClO^- from 0 to 20 μM, the absorption intensity was a linear function with ClO^- (Fig. 3a, inset, R 0.999). The absorption intensity at 533 nm increased by 97-fold, and its molar extinction coefficient increased from 3.5×10^2 to 3.4×10^4 L●mol^{-1}●cm^{-1}. As addition of ClO^- over time, the fluorescent intensity of 6G-ClO strengthened continuously at 556 nm (Fig. 3b). A linear function of emission intensity at 556 nm related to ClO^- concentration range from 0 to 10 μM was built

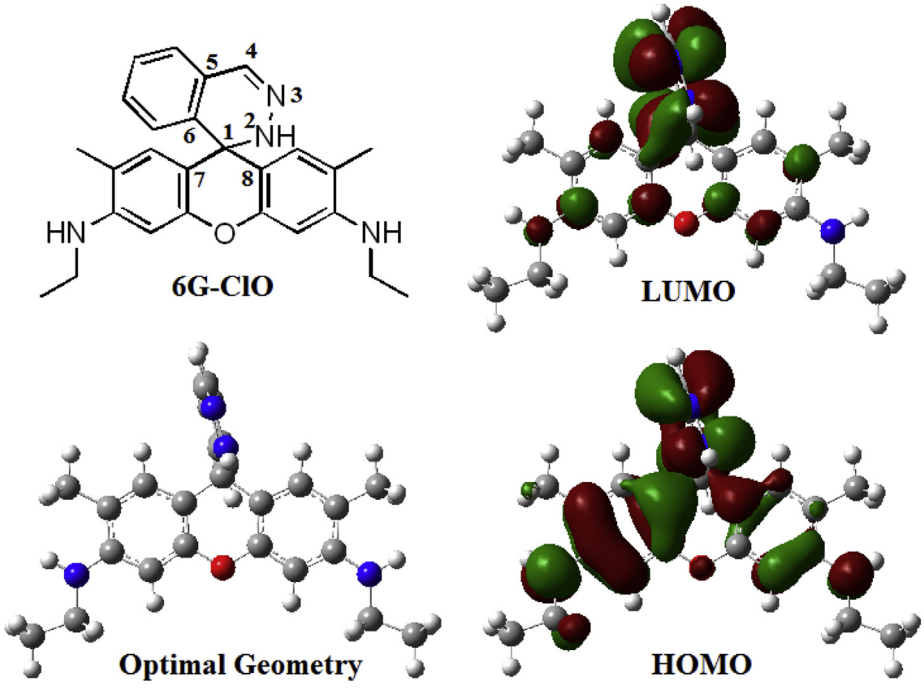

Fig. 1. The geometry and frontier molecular orbitals (HOMO and LUMO) of 6G-ClO optimized by DFT/B3LYP/6-31G(d) level.

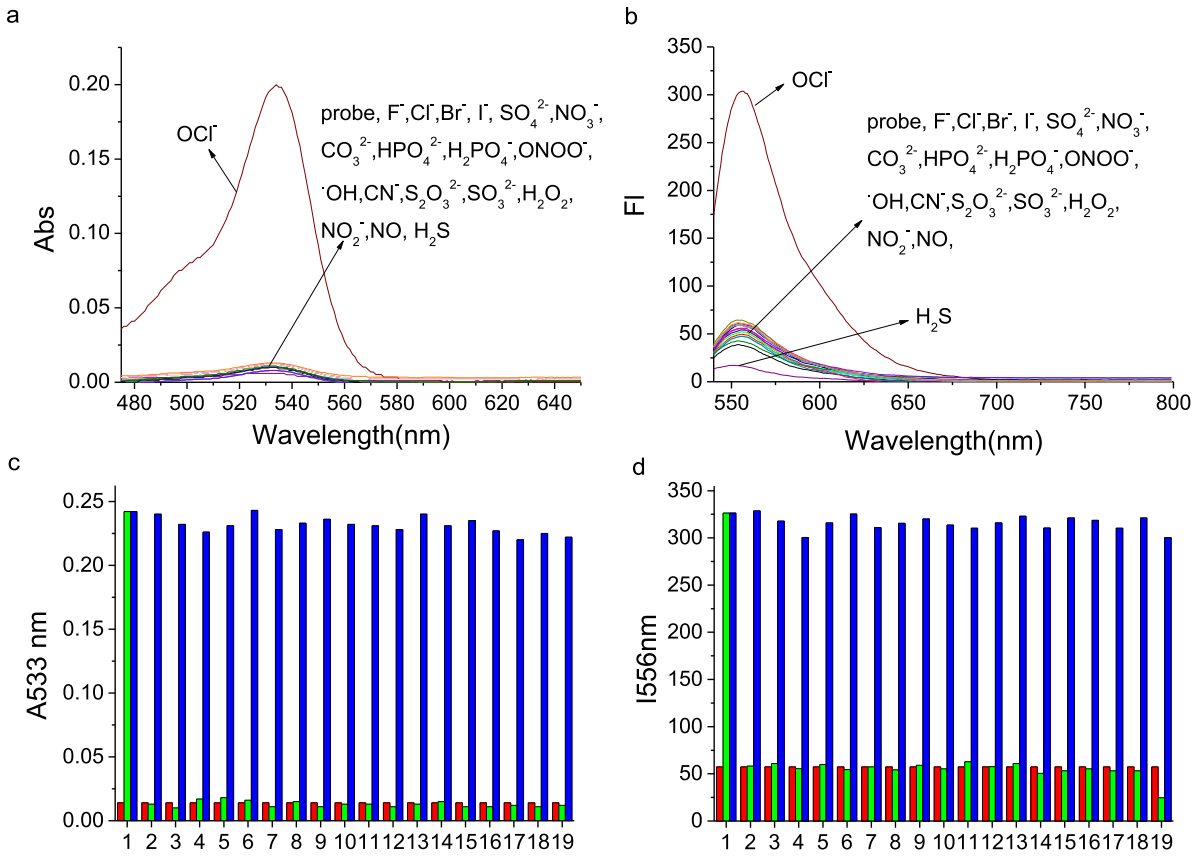

Fig. 2. Absorption (a) and emission (b) spectra of 6G-ClO in C_2H_5OH/HEPES (v/v 1/1, pH 7.4) in the presence of various anions (5 equiv.). The maximum of absorption (c) and emission (d) of 6G-ClO in the presence of various anions (5 equiv.). Red bars represent the solution of 6G-ClO in C_2H_5OH/HEPES (v/v 1/1, pH 7.4). Green bars represent the addition of various anions, respectively. Blue bars represent the subsequent addition of ClO^-. 1. ClO^-, 2. $ONOO^-$, 3. Cl^-, 4. HPO_4^{2-}, 5. $H_2PO_4^-$, 6. SO_4^{2-}, 7. NO_3^-, 8. CO_3^{2-}, 9. $S_2O_3^{2-}$, 10. H_2O_2, 11. NO_2^-, 12. ·OH, 13. F^-, 14. SO_3^{2-}, 15. Br^-, 16. I^-, 17. CN^-, 18. NO, 19H_2S. (For interpretation of the references to color in this figure legend, the reader is referred to the Web version of this article.)

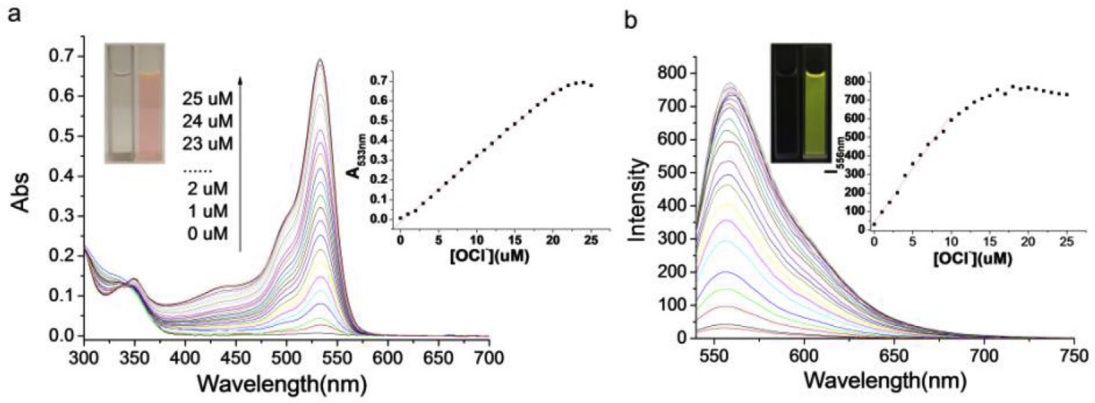

Fig. 3. The absorption (a) and emission (b) changes of 6G-ClO (2×10^{-5} M) in C_2H_5OH/HEPES (v/v 1:1, pH 7.4) upon addition of ClO^-. Inset: the absorption intensity at 533 nm and emission intensity at 556 nm versus the different concentration of ClO^-, respectively.

(Fig. 3b, inset, R 0.991). 6G-ClO showed a 30-fold enhancement of fluorescence intensity at 556 nm, and the maximum of fluorescence quantum yield was up to 0.68 in the solution. The detection limit was calculated by titration data, according to the triple signal-to-noise ratio method [65]. The detection limit of 6G-ClO for ClO^- is determined to be 26 nM and 12 nM, corresponding to the absorption and emission spectra. Upon addition of 120 μM ClO^- into 6G-AH solution, the molar extinction coefficient of 6G-AH solution only increased up to 1.3×10^4 L●mol^{-1}●cm^{-1}. The lower slope of linear function of titration of 6G-AH suggested that the sensitivity of 6G-AH for hypochlorite was inferior to that of 6G-ClO (Fig. S3). As expected, six-membered 6G-ClO could be used as a highly sensitive fluorescent probe for ClO^- detection.

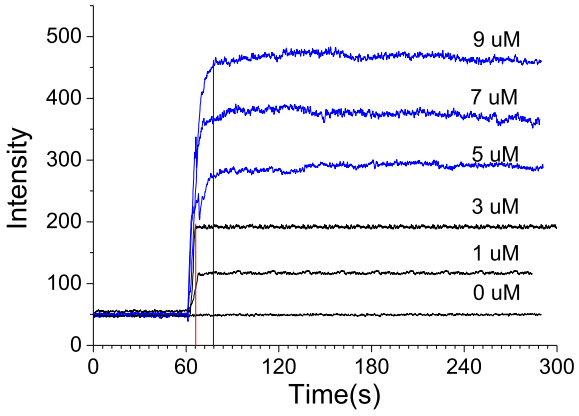

Fig. 4. Intensity changes of 6G-ClO (2×10^{-5} M) at 556 nm upon addition of ClO^-, such as 0, 1, 3, 5, 7, 9 μM.

3.5. Kinetic analysis of 6G-ClO towards ClO^-

Time-dependent fluorescence of 6G-ClO was monitored in absence and presence of ClO^-, as shown in Fig. 4. In the absence of ClO^-, fluorescent intensity at 556 nm of 6G-ClO solution was very faint and stable, under excitation exposure at 525 nm for 5 min and 60 min (Fig. S4). When low concentration of ClO^- (1, 3 μM) was added into 6G-ClO solution, the intensity of 6G-ClO achieved the maximum within 6 s, and didn't distinctly fluctuate in the following test process. When 5, 7 or 9 μM ClO^- was added, the intensity of 6G-ClO achieved the maximum within 18 s and then leveled off. The fast response of 6G-ClO towards ClO^- suggested that the high electron density in six-membered rhodamine hydrazone moiety might play vital roles in the oxidation between 6G-ClO and hypochlorite anion.

3.6. pH effect

The spectral changes of 6G-ClO with different pH values were tested, as shown in Fig. 5. In the absence of ClO^-, there were similar trends for absorption and emission spectra at different pH values. The absorption and emission peaks of 6G-ClO was very faint above pH 6.0, which signified stable six-membered rhodamine hydrazone form in 6G-ClO. With pH decreasing, both absorption and emission were gradually enhanced, suggesting that six-membered spirocycle in 6G-ClO underwent a ring-opening reaction in the process of protonation of 6G-ClO. The pH titration data provided pKa value of probe 6G-ClO as 2.07 (±0.06) (Abs) and 2.62 (±0.14) (Fl), respectively (Figs. 5a and 4b). After 1 equiv. ClO^- was added into 6G-ClO solution, the absorption and emission spectra of this mixture did not change over a pH range from 3.5 to 8.0.

3.7. Response mechanism of 6G-ClO with ClO^-

ClO^- could oxidize hydrazone moiety in 6G-ClO and induce a ring-opening reaction of six-membered rhodamine hydrazone spirocycle [66]. In order to confirm the product of ring-opening reaction of 6G-ClO, the composition of 6G-ClO and ClO^- mixtures were analyzed in mass spectra (Fig. S5). A new peak at *m/z* 447.20 (N—Cl) was found in mass spectrum, upon addition of ClO^- into 6G-ClO in methanol. The ratio of mass and charge at *m/z* 447.20 was 35 more than that of 6G-ClO (Found *m/z* 412.20). Moreover, by comparing the isotope abundance, it was speculated that there was a chlorination of hydrazone in 6G-ClO (N—Cl *m/z* 447.19), as shown in Scheme 2. In the presence of water, the N—Cl intermediate would

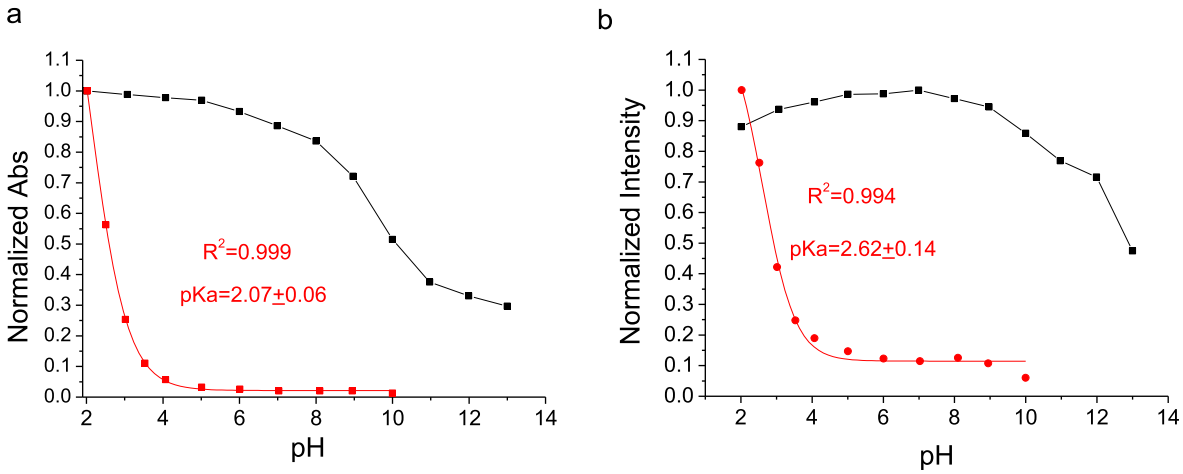

Fig. 5. The normalized absorption (a) and emission (b) intensity with maximum of 6G-ClO in the absence (red cycle) and presence (black square) of 1.0 equiv. ClO^- in C_2H_5OH/H_2O (1:1 v/v) versus different pH values. (For interpretation of the references to color in this figure legend, the reader is referred to the Web version of this article.)

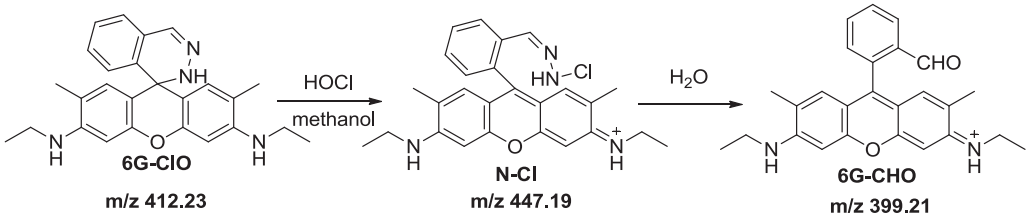

Scheme 2. Proposed mechanism of 6G-ClO with ClO^-

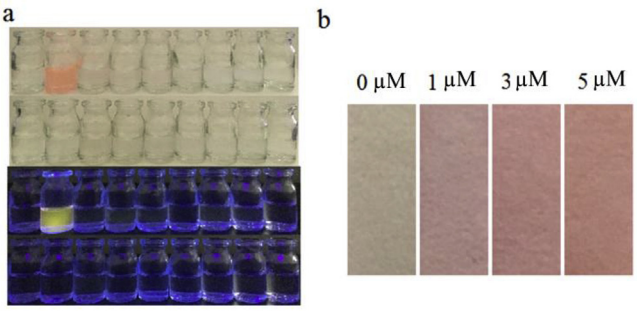

Fig. 6. (a) Absorption and emission color changed when 20 μM ClO^- was added into the vials containing various anions, respectively. (b) Test papers soaked with 6G-ClO (50 μM, in CH_2Cl_2) was immersed in 0, 1, 3 and 5 μM NaClO solution, respectively. (For interpretation of the references to color in this figure legend, the reader is referred to the Web version of this article.)

Table 1
The ClO^- concentration in tap water and swimming pool water.

S[a]	$[\overline{ClO}]$[b] (μM)		Found (μM)			Average (μM)	Recovery%
			n = 1	n = 2	n = 3		
S1	3.02	Abs	3.05	3.18	3.16	3.13 ± 0.06	103.6%
		Fl	2.93	2.89	3.00	2.94 ± 0.05	97.4%
S2	3.60	Abs	3.82	3.83	3.72	3.79 ± 0.05	105.3%
		Fl	3.72	3.52	3.77	3.67 ± 0.11	101.9%

[a] S1 is tap water from student dorm, Liaoning University. S2 is swimming pool water from Liaoning University.
[b] [ClO^-]is the concentration of sample calibrated by standard method.

be further hydrolyzed into 6G-CHO (Found *m*/*z* 399.23). The final product of 6G-ClO with ClO^- was purified by column chromatography, and characterized by ^1H NMR spectra. Compared with 6G-CHO, it can be confirmed that the final product of 6 G-ClO with ClO^- was 6G-CHO (Fig. S6). Therefore, a response mechanism was proposed that ClO^- could chloridize rhodamine hydrazone and induce ring-opening in the six-member of 6G-ClO (Scheme 2).

3.8. Qualitative and quantitative detection for ClO^- in water

The color changes and "off-on" fluorescence of 6G-ClO provided superior qualitative and quantitative method for ClO^- detection. As shown in Fig. 6a, 6G-ClO can recognize the vials containing ClO^-, after it was injected into each vial. Pink color and yellow-green fluorescence appearance meant that the solution must contain ClO^- in that vial. To semiquantitatively detect ClO^- in vial, test-strips were prepared and used to monitor ClO^- in the solution. Test strips were immersed respectively into the solution with various concentration of ClO^- (0, 1, 3, 5 μM) for 30 s. The color of test strips deepened with the increasing concentration of hypochlorite solutions (Fig. 6b). Subsequently, standard curve method was used to quantitatively probe ClO^- in the solution. As shown in Table 1, the concentration of ClO^- in water was 3.02 and 3.6 μM, respectively, calibrated by methods reported in literature [60,61]. Assessed by the standard curve, the concentration of ClO^- both tap water and swimming pool water was measured by 3 times. The average ClO^- concentration of tap water and swimming pool water was 3.13 μM and 3.79 μM, respectively, calculated by the standard curve of absorption. According to the standard curve of emission, 2.94 μM ClO^- in tap water and 3.67 μM ClO^- in swimming pool water were found. Recoveries ranging from 97.4% to 105.3% indicated that 6G-ClO, as a colorimetric and fluorometric probe, had good accuracy in quantitative hypochlorite detection in aqueous solution.

3.9. Exogenous/endogenous ClO^- imaging of 6G-ClO in living lysosomes

Before applied cell imaging, the cytotoxic effect of 6G-ClO on HUVEC cells was evaluated by using MTT assay (Fig. S7). When HUVEC cells in cell growth logarithmic phase was treated with 6G-ClO (0–10 μM) for 24 h, the cell viabilities were higher than 90%, which suggested that 6G-ClO had low cytotoxicity within the concentration range from 1 to 5 μM. The low cytotoxicity of 6G-ClO would be well suited for bio-imaging of HUVEC cells. HUVEC cells, a kind of endothelial cells, were used as cell model for endogenic nitric oxide or hypochlorite generation stimulated by LPS in the process of oxidative stress. Herein, HUVEC cells were chosen in the co-localization study and exogenous hypochlorite monitoring. The co-localization study of HUVEC cells stained with 6G-ClO was implemented to confirm its organelle-specifity. HUVEC cells were incubated with 6G-ClO for 10 min, and then 1 μM ClO^- was added. These cells glowed with red discrete fluorescence in subcellular locations, upon excitation at 488 nm (Fig. S8). As we know, rhodamine dyes are liable to accumulate in mitochondria of living cells. Then Mito-tracker Deep Red was used as a reference to verify the mitochondrion-specifity of 6G-ClO (Fig. S9). There was no overlap in the merged imaging for Ch1 and Ch 2, whose Pearson's coefficient and Mander's overlap coefficient were very low. The skewed hourglass shapes of ICA plot further indicated that 6G-ClO did not accumulate in mitochondria of HUVEC cells. To further determine the organelles with red fluorescence, these cells were further stained with lysosome tracker (DND-26). As shown in Fig. 7, HUVEC cells stained with DND-26 and 6G-ClO (ClO^-) exhibited green and red fluorescence in Channel 1 (Ch1) and 2 (Ch2), respectively. The merged image of DIC, Ch1 and Ch2 demonstrated that green and red fluorescence overlaid well within the cells (Fig. 7a). The high Pearson's coefficient (0.94) and Mander's overlap coefficient (0.96) indicated that 6G-ClO can specifically accumulate in lysosomes of HUVEC cells. The intensity scatter plot showed diagonal distribution between Ch1 and Ch2, indicated that 6G-ClO and DND-26 possessed similar localization and intensity distribution in lysosomes (Fig. 7b). Moreover, skewed hourglass shapes of ICA plot with positive values further verified that there was a dependent intensity distribution between Ch1 and Ch2 (Fig. 7c). These results demonstrated that 6G-ClO used as a nondestructive probe can monitor exogenous hypochlorite in lysosomes of HUVEC cells.

In order to monitor endogenous hypochlorite anion in living cells, HUVEC cells were incubated with 6G-ClO in the absence and presence of Lipopolysaccharide (LPS) for 24 h at 37 °C. As shown in Fig. 8a (1), there was a faint fluorescence in HUVEC cells without stimulant LPS. To determine whether the fluorescence was induced by endogenous hypochlorite in absence of LPS, a comparative test to treat cells with myeloperoxidase inhibitor (4-aminobenzoic acid hydrazide (4-ABAH)) has been implemented (Fig. S10). In the control group, there was a faint fluorescence in HUVEC cells stained with 6G-ClO. Compared with control cells, the fluorescent intensity of cells inhibited by 4-ABAH did not decline obviously, which indicated the faint fluorescence in control group was not caused by a small amount of endogenous ClO^- in lysosomes of living cells. Additionally, it was not observed an enhancement of intensity in control group during the excitation at 515 nm in the microscope (Fig. S11). Stimulated with LPS, a significant enhancement of

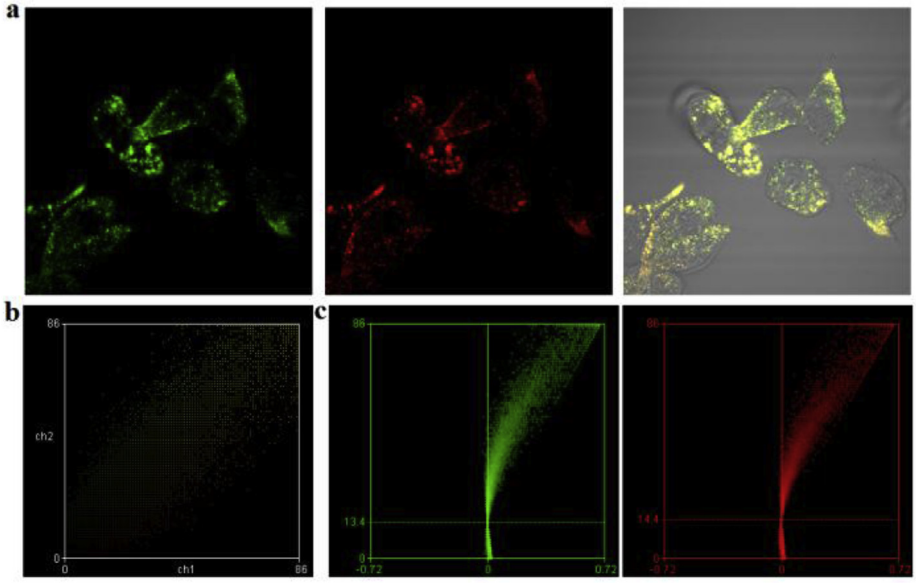

Fig. 7. (a) The images of Green Channel, Red Channel and overlays of Green Channel, Red Channel and differential interference contrast (DIC). Green channel: fluorescent image of HUVEC cells stained with Lyso-tracker DND-26 (2 μM), λex 405 nm, λem 480–500 nm. Red channel: fluorescent image of HUVEC cells stained with 6G-ClO (2 μM), λex 488 nm, λem 550–650 nm. (b) Intensity correlation plot of Green and Red Channel. (c) Intensity correlation analysis (ICA) plot of Green Channel and Red Channel, respectively. (For interpretation of the references to color in this figure legend, the reader is referred to the Web version of this article.)

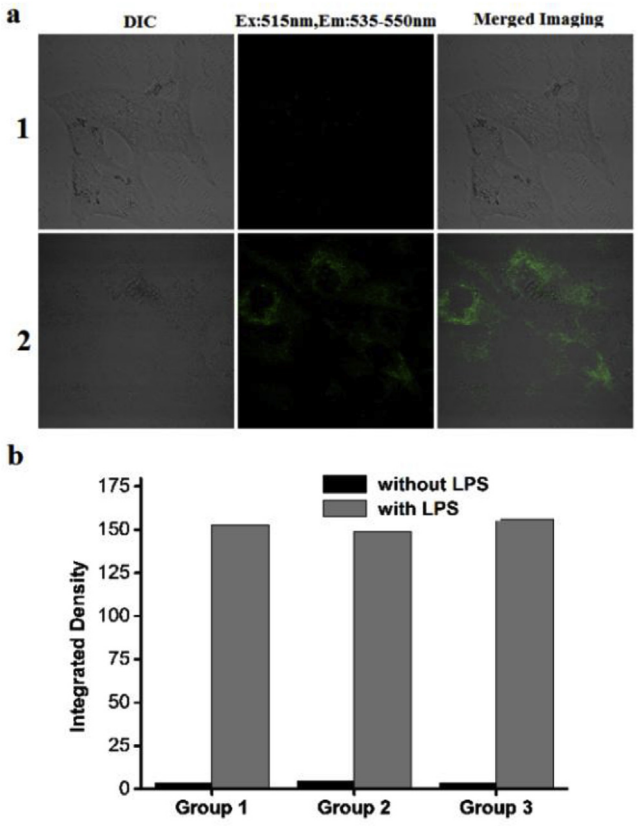

Fig. 8. (a) Fluorescent images of HUVEC cells stained with probe 6G-ClO and further stimulated with LPS. 1 is the control group. 2 is the experimental group. (b) The integrated density of HUVEC cells stimulated with or without LPS.

fluorescence intensity was observed in lysosomes of HUVEC cells (Fig. 8a (2)), which should be attributed to the generation of endogenous hypochlorite stimulated by LPS. In order to quantitatively illuminate the enhancement of fluorescent intensity in cells with/without LPS, the integrated intensity and optical density of cells was assessed with the aid of Image J (Fig. S12, Tab S1). Compared with control group, the integrated intensity of cells stimulated by LPS increased visibly (Fig. 8b). The average optical density of cells in stimulated group was in the range from $(2.38–3.68) \times 10^{-2}$/pixel, which was nearly twice as high as that of cells in control groups ($(1.12–1.77) \times 10^{-2}$/pixel). These results demonstrated that 6G-ClO could be an excellent lysosome targetable fluorescent probe practically applicable to monitor endogenous ClO^- in living HUVEC cells.

4. Conclusion

In summary, to construct new hypochlorite probe based on six-membered rhodamine spirocycles, a rhodamine platform (6G-CHO) bearing formyl group in 2-position was firstly developed via the reduction of rhodamine 6G spiroaminoethanol with $LiAlH_4$. Hypochlorite probe 6G-ClO can be easily synthesized and confirmed by the chemical shift of spiro-carbon (δ_C 94.9 ppm) and −CH═N−NH (δ_{CH} 8.03 ppm; δ_{NH} 6.51 ppm) in NMR spectra.. Compared with 6G-AH, twist six-membered spirocycle of 6G-ClO optimized by Gaussian software at DFT/B3LYP/6-31G(d) level would be beneficial to the selectivity and sensitivity of fluorescent probe for hypochlorite. The high selectivity of probe 6G-ClO manifested 6G-ClO can qualitatively detect the hypochlorite existing in solution without interference from the other anions and metal ions. 6G-ClO with high sensitivity can quantitatively monitor the concentration of hypochlorite in real water samples such as tap water and swimming pool water. The detection limit of 6G-ClO was 12 nM, calculated by the triple signal-to-noise ratio methods. Moreover, 6G-ClO displayed fast response towards hypochlorite (6–18s). The co-localization staining of HUVEC cells further verified that 6G-ClO could specifically localize in lysosomes of living cells. In addition, 6G-ClO with low cytotoxicity also can capture endogenous ClO^- in lysosomes stimulated by LPS. These results suggested that the new six-membered rhodamine spirocyclic hydrazone for hypochlorite

detection would lead to the opportunities not only for determining ClO^- in water and biological samples, but also for the evaluation of oxidation stress induced by pollutants.

Declaration of interest statement

The authors declare no conflicts of interest.

Declaration of competing interest

☑The authors declare that they have no known competing financialinterestsor personal relationships that could have appeared to influence the work reported in this paper.

Acknowledgments

This work was supported by Natural Science Foundation of Liaoning Province, China (20180510044), National Natural Science Foundation of China (No. 21302080, No. 31600311), Liaoning University Students' Innovation and Entrepreneurship Training Program (x201810140183) and Program Funded by Liaoning Province Education Administration, China (No. L2014010).

Appendix A. Supplementary data

Supplementary data to this article can be found online at https://doi.org/10.1016/j.aca.2019.07.046.

References

[1] P.K. Roy, D. Kumar, M. Ghosh, A. Majumder, Disinfection of water by various techniques-comparison based on experimental investigations, Desalin Water Treat 57 (2016) 28141–28150.
[2] J.Q. Jiang, B. Lloyd, Progress in the development and use of ferrate (VI) salt as an oxidant and coagulant for water and wastewater treatment, Water Res. 36 (2002) 1397–1408.
[3] S. Fukuzaki, Mechanisms of actions of sodium hypochlorite in cleaning and disinfection processes, Biocontrol Sci. 11 (2006) 147–157.
[4] R.X. Yuan, S.N. Ramjaun, Z.H. Wang, J.S. Liu, Effects of chloride ion on degradation of acid orange 7 by sulfate radical-based advanced oxidation process: implications for formation of chlorinated aromatic compounds, J. Hazard Mater. 196 (2011) 173–179.
[5] S.T. Chang, M.S. Chou, H.Y. Chang, Elimination of odors emitted from hot-melting of recycle ps by oxidative-reductive scrubbing, Aerosol Air Qual. Res. 14 (2014) 293–300.
[6] M.K. Bruch, Toxicity and safety of topical sodium hypochlorite, Contrib. Nephrol. 154 (2007) 24–38.
[7] H.D. Dakin, On the use of certain antiseptic substances in the treatment of infected wounds, Br. Med. J. 2 (1915) 318–320.
[8] M. Haapasalo, Y. Shen, W. Qian, Y. Gao, Irrigation in endodontics, dent, Clin. N. Am. 54 (2010) 291–312.
[9] J.F. Siqueira Jr., I.N. Rocas, A. Favieri, K.C. Lima, Chemomechanical reduction of the bacterial population in the root canal after instrumentation and irrigation with 1%, 2.5%, and 5.25% sodium hypochlorite, J. Endod. 26 (2000) 331–334.
[10] W.A. Rutala, D.J. Weber, Uses of inorganic hypochlorite (bleach) in health-care facilities, Clin. Microbiol. Rev. 10 (1997) 597–610.
[11] J. Koivunen, H. Heinonen-Tanski, Inactivation of enteric microorganisms with chemical disinfectants, UV irradiation and combined chemical/UV treatments, Water Res. 39 (2005) 1519–1526.
[12] A. Breytus, A.P. Kruzic, S. Prabakap, Chlorine decay and chlorate formation in two water treatment facilities, J. AWWA (Am. Water Works Assoc.) 109 (2017) 110–120.
[13] Z.T. How, I. Kristiana, F. Busetti, K.L. Linge, C.A. Joll, Organic chloramines in chlorine-based disinfected water systems: a critical review, J. Environ. Sci. 58 (2017) 2–18.
[14] B.D. Stanford, A.N. Pisarenko, S.A. Snyder, G. Gordon, Perchlorate, bromate and chlorate in hypochlorite solutions: guidelines for utilities, J. AWWA (Am. Water Works Assoc.) 103 (2011) 71–83.
[15] G. Gordon, L.C. Adam, B.P. Bubnis, C. Kuo, R.S. Cushing, R.H. Sakaji, Predicting liquid bleach decomposition, J. AWWA (Am. Water Works Assoc.) 89 (1997) 142–149.
[16] M.J. Nieuwenhuijsen, R. Smith, S. Golfinopoulos, N. Best, J. Bennett, G. Aggazzotti, E. Righi, G. Fantuzzi, L. Bucchini, S. Cordier, Health impacts of long-term exposure to disinfection by-products in drinking water in Europe: HIWATE, J. Water Health 7 (2009) 185–207.
[17] T.J. Woodruff, A. Carlson, J.M. Schwartz, L.C. Giudice, Proceedings of the summit on environmental challenges to reproductive health and fertility: executive summary, Fertil. Steril. 89 (2008) 281–300.
[18] H. Jaeschke, Reactive oxygen and mechanisms of inflammatory liver injury: present concepts, J. Gastroenterol. Hepatol. 26 (1) (2011) 173–179.
[19] A. Strzepa, K.A. Pritchard, B.N. Dittel Myeloperoxidase, A new player in autoimmunity, Cell. Immunol. 317 (2017) 1–8.
[20] O.M. Panasenko, The mechanism of the hypochlorite-induced lipid peroxidation, Biofactors 6 (1997) 181–190.
[21] C.L. Hawkins, D.I. Pattison, M.J. Davies, Hypochlorite-induced oxidation of amino acids, peptides and proteins, Amino Acids 25 (2003) 259–274.
[22] S.M. Wu, S.V. Pizzo, α_2-Macroglobulin from rheumatoid arthritis synovial fluid: functional analysis defines a role for oxidation in iflammation arch biochem biophys, Arch. Biochem. Biophys. 391 (2001) 119–126.
[23] E. Malle, T. Buch, H.J. Grone, Myeloperoxidase in kidney disease, Kidney Int. 64 (2003) 1956–1967.
[24] S. Hammerschmidt, N. Buchler, H. Wahn, Tissue lipid peroxidation and reduced glutathione depletion in hypochlorite-induced lung injury, Chest 121 (2002) 573–581.
[25] C. Bergt, S. Pennathur, X.Y. Fu, J. Byun, K. O'Brien, T.O. McDonald, P. Singh, G.M. Anantharamaiah, A. Chait, J. Brunzell, R.L. Geary, J.F. Oram, J.W. Heinecke, The myeloperoxidase product hypochlorous acid oxidizes HDL in the human artery wall and impairs ABCA1-dependent cholesterol transport, Proc. Natl. Acad. Sci. 101 (2004) 13032–13037.
[26] R. Rao, Oxidative stress-induced disruption of epithelial and endothelial tight junctions, Front. Biosci. 13 (2008) 7210–7226.
[27] W.L. Wu, H.L. Ma, L.L. Xi, M.F. Huang, K.M. Wang, J.Y. Miao, B.X. Zhao, A novel lipid dropletstargeting ratiometric fluorescence probe for hypochlorous acid in living cells, Talanta 194 (2019) 308–313.
[28] Y. Pak, S.J. Park, Q.L. Xu, H.M. Kim, J. Yoon, A ratiometric two-photon fluorescent probe for detecting and imaging hypochlorite, Anal. Chem. 90 (2018) 9510–9514.
[29] L.L. Wu, Q.Y. Yang, L.Y. Liu, A.C. Sedgwick, A.J. Cresswell, S.D. Bull, C. Huang, T.D. James, An ESIPT-based fluorescence probe for the rapid detection of hypochlorite (HOCl/ClO^-), Chem. Commun. 54 (2018) 8522–8525.
[30] X. Lv, X. Yuan, Y. Wang, W. Guo, A naphthalimide based fast and selective fluorescent probe for hypochlorous acid/hypochlorite and its application for bioimaging, New J. Chem. 42 (2018) 15105–15110.
[31] M.P. Algi, A highly selective dual channel hypochlorite probe based on fluorescein and 1,10-phenanthroline, Tetrahedron 72 (2016) 1558–1565.
[32] W.L. Wu, X. Zhao, L.L. Xi, M.F. Huang, W.H. Zeng, J.Y. Miao, B.X. Zhao, A mitochondria-targeted fluorescence probe for ratiometric detection of endogenous hypochlorite in the living cells, Anal. Chim. Acta 950 (2017) 178–183.
[33] W.Y. Lin, L.L. Long, B.B. Chen, W. Tan, A ratiometric fluorescent probe for hypochlorite based on a deoximation reaction, Chem. Eur J. 15 (2010) 2305–2309.
[34] P.P. Peng, H. Li, L. Bai, L.L. Wang, B.X. Chen, C.M. Yu, C.W. Zhang, J.Y. Ge, L. Li, W. Huang, Photocontrollable fluorogenic probe for visualizing near-membrane hypochlorite in live cells, Chemistry 3 (2018) 5981–5986.
[35] X. Tang, Z. Zhua, Y. Wang, J. Han, L. Ni, H.Q. Zhang, J. Li, Y.L. Mao, A cyanobiphenyl based fluorescent probe for rapid and specific detection of hypochlorite and its bio-imaging applications, Sens. Actuators B Chem. 262 (2018) 57–63.
[36] S.L. Shen, X.Q. Huang, X.H. Lin, X.Q. Cao, A ratiometric fluorescent probe for lysosomal hypochlorous acid based on through-bond energy transfer strategy, Anal. Chim. Acta 1052 (2019) 124–130.
[37] S. Das, K. Aich, L. Patra, K. Ghoshal, S. Gharami, M. Bhattacharyya, T.K. Mondal, Development of a new fluorescence ratiometric switch for endogenous hypochlorite detection in monocytes of diabetic subjects by dye release method, Tetrahedron Lett. 59 (2018) 1130–1135.
[38] K.M. Xiong, F.J. Huo, Y.B. Zhang, Y. Wen, J.B. Chao, C.X. Yin, A novel recognition mechanism based on aldehyde group oxidized into carboxyl group by hypochlorite for the materials of fluorescent probes, Sens. Actuators B Chem. 224 (2016) 307–314.
[39] L. Long, D. Zhang, X. Li, J. Zhang, C. Zhang, L. Zhou, A fluorescence ratiometric sensor for hypochlorite based on a novel dual-fluorophore response approach, Anal. Chim. Acta 775 (2013) 100–105.
[40] H.N. Kim, M.H. Lee, H.J. Kim, J.S. Kim, J. Yoon, A new trend in rhodamine-based chemosensors: application of spirolactam ring-opening to sensing ions, Chem. Soc. Rev. 37 (2008) 1465–1472.
[41] Y. Xia, X. Liu, D. Wang, Z. Wang, Q. Liu, H. Yu, M. Zhang, Y. Song, A fluorometric and mitochondrion-targetable probe for rapid, naked-eye test of hypochlorite in real samples, Chin. Chem. Lett. 29 (2018) 1517–1520.
[42] Y. Sun, F. Ding, Z.X. Zhou, C.L. Li, M.P. Pu, Y.L. Xu, Y.B. Zhan, X.J. Lu, H.B. Li, G.F. Yang, Y. Sun, P.J. Stang, Rhomboidal Pt(II) metallacycle-based NIR-II theranostic nanoprobe for tumor diagnosis and imageguided therapy, Proc. Natl. Acad. Sci. U.S.A. 116 (2019) 1968–1974.
[43] Y. Sun, S. Chen, X.Y. Chen, Y.L. Xu, S.Y. Zhang, Q.Y. Ouyang, G.F. Yang, H.B. Li, A highly selective and recyclable NO-responsive nanochannel based on a spiroring opening-closing reaction strategy, Nat. Commun. 10 (2019) 1323–1330.
[44] F. Ding, Y. Fan, Y. Sun, F. Zhang, Beyond 1000 nm emission wavelength: recent advances in organic and inorganic emitters for deep-tissue molecular imaging, Adv. Healthc. Mater. (1–15) (2019) 1900260.

[45] F. Ding, Y.B. Zhan, X.J. Lu, Y. Sun, Recent advances in near-infrared II fluorophores for multifunctional biomedical imaging, Chem. Sci. 9 (2018) 4370–4380.
[46] Y. Sun, X.D. Zeng, Y.L. Xiao, C.H. Liu, H. Zhu, H. Zhou, Z.Y. Chen, F.C. Xu, J.L. Wang, M.Y. Zhu, J.Z. Wu, M. Tian, H. Zhang, Z.X. Deng, Z. Cheng, X.C. Hong, Novel dual-function near-infrared II fluorescence and PET probe for tumor delineation and imageguided surgery, Chem. Sci. 9 (2018) 2092–2097.
[47] F. Ding, C.L. Li, Y.L. Xu, J.X. Li, H.B. Li, G.F. Yang, Y. Sun, Pegylation regulates self-assembled small-molecule dye-based probes from single molecule to nanoparticle size for multifunctional NIR-II bioimaging, Adv. Healthc. Mater. 7 (1–9) (2018) 1800973.
[48] Y.L. Xu, M. Tian, H. Zhang, Y.L. Xiao, X.C. Hong, Y. Sun, Recent development on peptide-based probes for multifunctional biomedical imaging, Chin. Chem. Lett. 29 (2018) 1093–1097.
[49] X. Chen, T. Pradhan, F. Wang, J.S. Kim, J. Yoon, Chemosensors based on spiroring-opening of xanthenes and related derivatives, Chem. Rev. 112 (2012) 1910–1956.
[50] Y. Sun, J. Liu, X. Lv, Y. Liu, Y. Zhao, W. Guo, Rhodamine-inspired far-red to near-infrared dyes and their application as fluorescence probes, Angew. Chem. Int. Ed. 51 (2012) 7634–7636.
[51] B.V. Shankar, A. Patnaik, A new pH and thermo-responsive chiral hydrogel for stimulated release, J. Phys. Chem. B 111 (2007) 9294–9300.
[52] V.P. Boyarskiy, V.N. Belov, R. Medda, B. Hein, M. Bossi, S.W. Hell Photostable, Amino reactive and water-soluble fluorescent labels based on sulfonated rhodamine with a rigidized xanthene fragment, Chem. Eur J. 14 (2008) 1784–1792.
[53] K. Kolmakov, V.N. Belov, J. Bierwagen, C. Ringemann, V. Muller, C. Eggeling, S.W. Hell, Red-emitting rhodamine dyes for fluorescence microscopy and nanoscopy, Chem. Eur J. 16 (2010) 158–166.
[54] M.K. Lee, P. Rai, J. Williams, R.J. Twieg, W.E. Moerner, Small-molecule labeling of live cell surfaces for three-dimensional super-resolution microscopy, J. Am. Chem. Soc. 136 (2014) 14003–14006.
[55] B. Biswal, D. Mallick, B. Bag, Signaling preferences of substituted pyrrole coupled six-membered rhodamine spirocyclic probes for Hg^{2+} ion detection, Org. Biomol. Chem. 14 (2016) 2241–2248.
[56] Z. Yang, L. Hao, B. Yin, M. She, M. Obst, A. Kappler, J. Li, Six-membered spirocycle triggered probe for visualizing Hg^{2+} in living cells and bacteria-EPS-mineral aggregates, Org. Lett. 15 (2013) 4334–4337.
[57] C. Wu, Q.N. Bian, B.G. Zhang, X. Cai, S.D. Zhang, H. Zheng, S.Y. Yang, Y.B. Jiang, Ring expansion of spiro-thiolactam in rhodamine scaffold: switching the recognition preference by adding one atom, Org. Lett. 14 (2012) 4198–4201.
[58] B. Wang, X. Cui, Z. Zhang, X. Chai, H. Ding, Q. Wu, Z. Guo, T. Wang, A six-membered-ring incorporated si-rhodamine for imaging of copper(ii) in lysosomes, Org. Biomol. Chem. 14 (2016) 6720–6728.
[59] A. Majumdar, C.S. Lim, H.M. Kim, K. Ghosh, New six-membered pH-insensitive rhodamine spirocycle in selective sensing of Cu^{2+} through C–C bond cleavage and its application in cell imaging, ACS Omega 2 (2017) 8167–8176.
[60] J.W.T. Spinks, The analysis of chlorine monoxide-chlorine mixtures, J. Am. Chem. Soc. 53 (1931) 3015–3016.
[61] M. Anbar, S. Guttmann, R. Rein, The isotopic exchange between hypohalites and halide ions. II. the exchangebetween hypochlorous acid and chloride lons, J. Am. Chem. Soc. 81 (1959) 1816–1821.
[62] Z. Wu, X. Wu, Z. Li, Y. Yang, J. Han, S. Han, Benzothiazoline based chemodosimeters for fluorogenic detection of hypochlorous acid, Bioorg. Med. Chem. Lett 23 (2013) 4354–4357.
[63] X. Hou, X. Guo, Z. Luo, H. Zhao, B. Chen, J. Zhao, J. Wang, A rhodamine-formaldehyde probe fluorescently discriminates H_2S from biothiols, Anal. Methods 6 (2014) 3223–3226.
[64] X. Wu, Z. Li, L. Yang, J. Han, S. Han, A self-referenced nanodosimeter for reaction based ratiometric imaging of hypochlorous acid in living cells, Chem. Sci. 4 (2013) 460–467.
[65] Z. Zhang, Y. Zou, C. Deng, L. Meng, A simple rhodamine hydrazide-based turn-on fluorescent probe for HOCl detection, Luminescence 31 (2016) 997–1004.
[66] H.L. Slates, D. Taub, C.H. Kuo, N.L. Wendler, Degradation of α-methyl-3,4-dihydroxyphenylalanine (α-methyldopa), J. Org. Chem. 29 (1964) 1424–1429.